Dohzono S Imai Y Nakamura H Wakitani S Takaoka K	Successful spinal fusion by E. coli-derived BMP-2-adsorbed porous beta-TCP granules: a pilot study. Successful spinal fusion by E. coli-derived BMP-2-adsorbed porous beta-TCP granules: a pilot study.	Clin Orthop Relat Res.	467	3206-3212	2009
Hoshino M Nakamura H Terai H Tsujio T Nabeta M Namikawa T Matsumura A Suzuki A Takayama K Takaoka K	Factors affecting neurological deficits and intractable back pain in patients with insufficient bone union following osteoporotic vertebral fracture.	Eur Spine J.	18(9)	1279-1286	2009
Suzuki A Misawa H Simogata M Tsutsumimoto T TakaokaK, Nakamura H.	Recovery Process Following Cervical Laminoplasty inPatients With Cervical Compression Myelopathy	Spine	34(26)	2874-2879	2009
松本守雄、長谷川徹、伊藤学、相澤俊峰、紺野慎一、山縣正庸、江原宗平、蜂谷裕道、中村博亮、八木省次、佐藤公昭、出沢明、吉田宗人、戸山芳昭、清水克時、永田見生	脊椎内視鏡下手術の現状 2008年1月～12月手術施行状況調査・インシデント報告集計結果.	日整会誌	83(12)	1022-1027	2009
松村昭、鈴木亨暢、堂園将、安田宏之、Najibullah Shafag、中村博亮	【腰椎手術における背筋にやさしい工夫】腰椎変性側弯症に対する顕微鏡視下片側進入両側除圧術後画像評価画像上の侵襲度評価	整形外科最小侵襲手術ジャーナル	53	55-62	2009

福永健治、岩城啓好、箕田行秀、池渕充彦、岡野匡志、渭川徹秀、飯田高広、橋本祐介、高岡邦夫、中村博亮.	MDCT を用いた人工股関節置換術後の DVT,PE の発生率の検討	日本関節病学会会誌	28(2)	213-217	2009
中村博亮、辻尾唯雄、寺井秀富、星野雅俊、豊田宏光、鈴木亨暢、伊達優子、高岡邦夫	骨粗鬆症性椎体骨折の治療　骨粗鬆症性椎体骨折偽関節発生の予測因子	Osteoporosis Japan	17 (2)	177-181	2009
中村博亮、辻尾唯雄、寺井秀富、星野雅俊、高岡邦夫	骨粗鬆症性脊椎骨折　診断、治療の最前線】骨粗鬆症性椎体骨折偽関節発生の予測因子	脊椎脊髄ジャーナル	22(3)	240-246	2009

Ⅳ. 研究成果の刊行物・別刷

Quick reference

骨粗鬆症性脊椎骨折に対する低侵襲vertebroplasty

日本大学医学部整形外科学　網代泰充
日本大学医学部整形外科学准教授　徳橋泰明
日本大学総合科学研究所教授　松崎浩巳

本術式の特徴

本術式の適応にはまだ議論はあるが，当科では適応・適応外を次のようにしている。

適応

①前方圧迫率50％以上の楔状圧迫型
②圧迫型，扁平破壊型で強い疼痛例

適応外

①alligator mouth型
②透析例

本術式は低侵襲に即時除痛と椎体の矯正を目的に，経椎弓根的にハイドロキシアパタイトブロック(以下，HAブロック)を充填する術式である。また，骨セメントやリン酸カルシウム骨ペーストと異なり，後壁損傷例での脊柱管内漏出や，経静脈的椎体外漏出による肺梗塞の危険がないきわめて安全な術式である。

手術手技

1 体位

体位は四点支持フレームを用いた腹臥位とする。この際，体位による骨折の整復を行うため，股関節は伸展位とする（**図1**）。

手術のコツ，注意点

整復されると骨折椎骨誤認の可能性があるため，必ず仙椎よりX線透視下にレベル確認をすること。

きれいで正確なX線透視が本法成功の最重要ポイントである。X線透視はスムーズに手術台下を移動でき，かつ患者の体に接触しないことが必要である。術前体位と透視の位置は重要なので，必ず術者自身が調整・確認すべきである。なお，X線透視の容易な移動のために手術台の支柱の位置は下肢側とする(**図2**)。

図1 体位

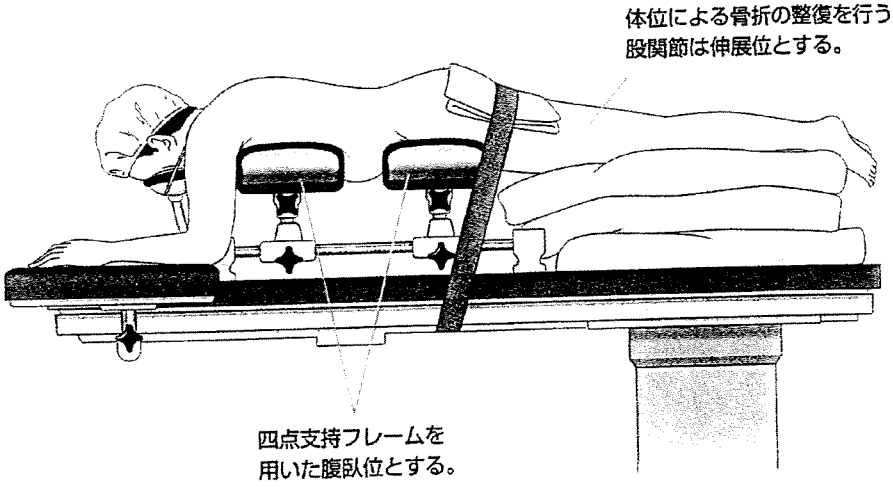
体位による骨折の整復を行うため，
股関節は伸展位とする。
四点支持フレームを
用いた腹臥位とする。

図2 X線透視

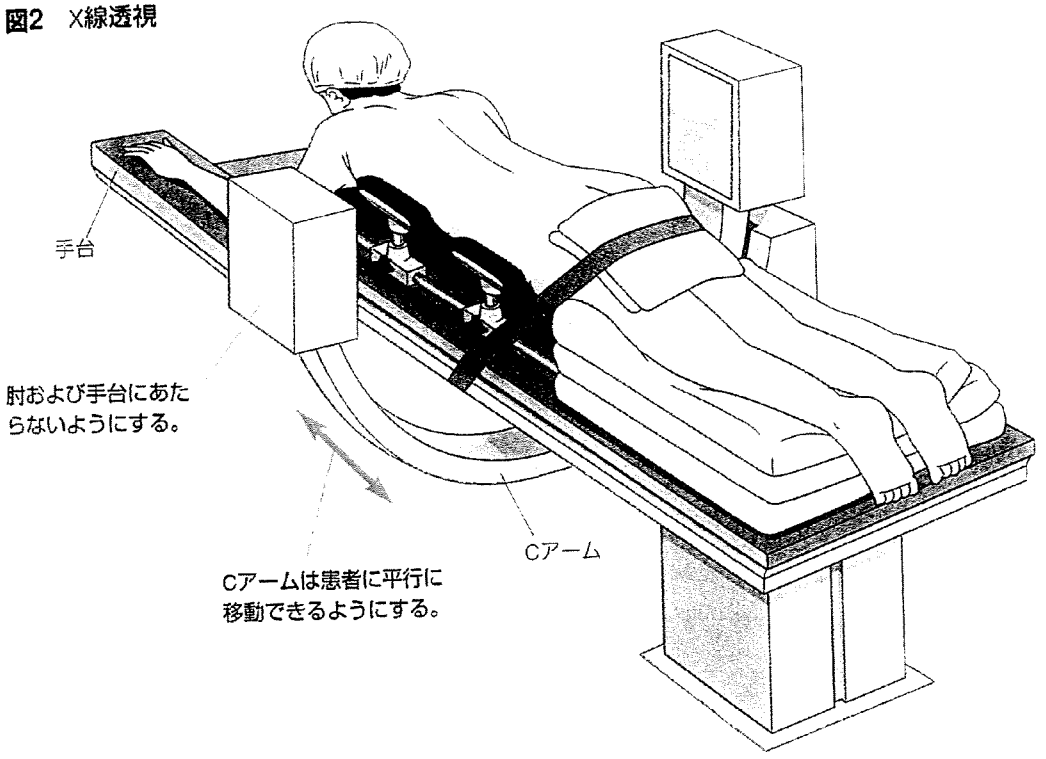
手台
肘および手台にあた
らないようにする。
Cアーム
Cアームは患者に平行に
移動できるようにする。

2 展開

棘突起から2～3cm外側(2横指外側)に約2cmの縦切開を加える(**図3**)。筋膜を先刃で縦切開し，筋肉を指またはエレバトリウムで鈍的に縦に分け，椎弓根に達する(**図4**)。

図3 皮切

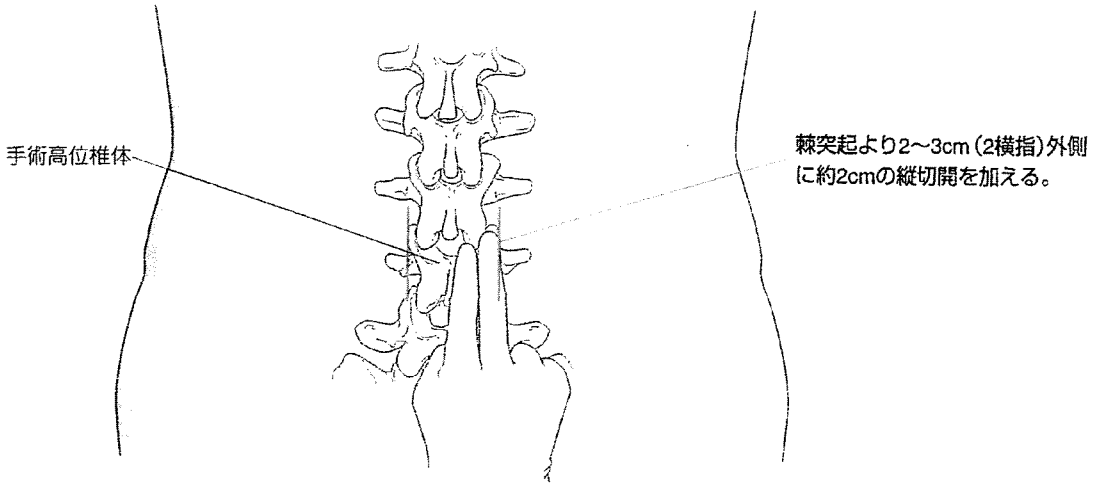

図4 椎弓根へのアプローチ

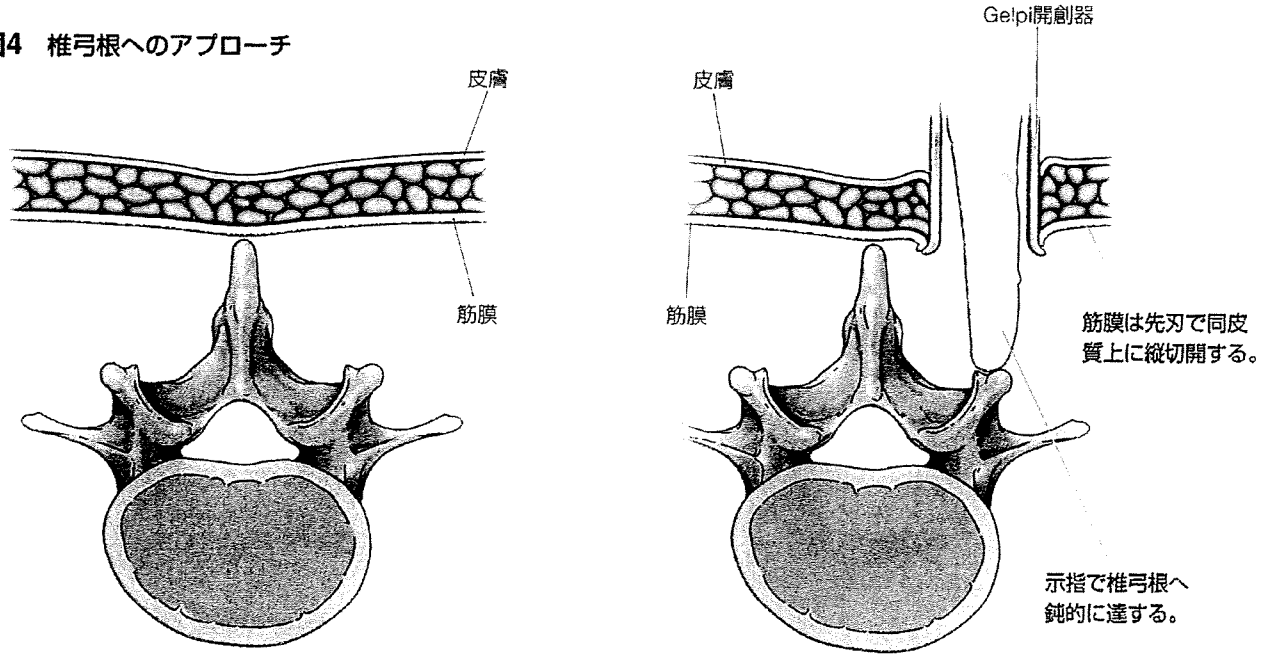

3 充填孔の作製

ペディクルスクリュー挿入操作と基本的には同様である。X線透視下にオウル，プローブなどで充填孔のスタート孔を作製する(**図5**)。この際，椎体中央に向け作製する。ガイド棒を4，5，6mm径と順次挿入して充填孔を拡大する。

手術のコツ，注意点

ガイド棒の挿入の深さもX線透視下に確認し，椎体中央の1/3までとする(**図6**)。

図5　充填孔の作製

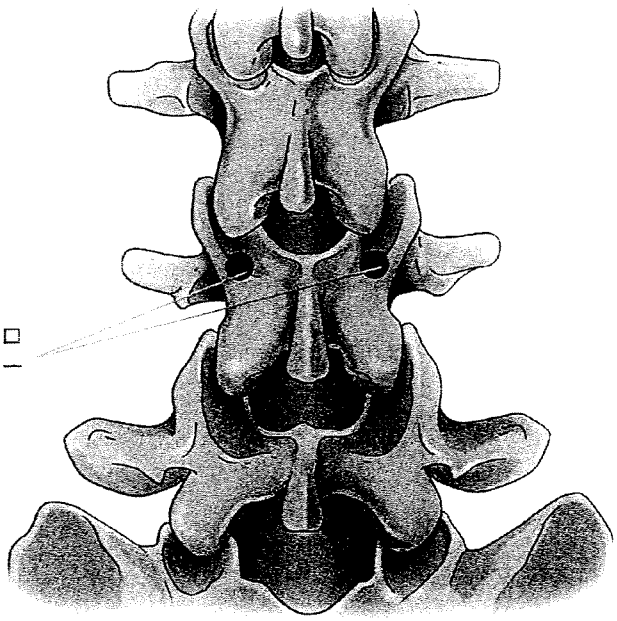

図6　HAブロックの挿入

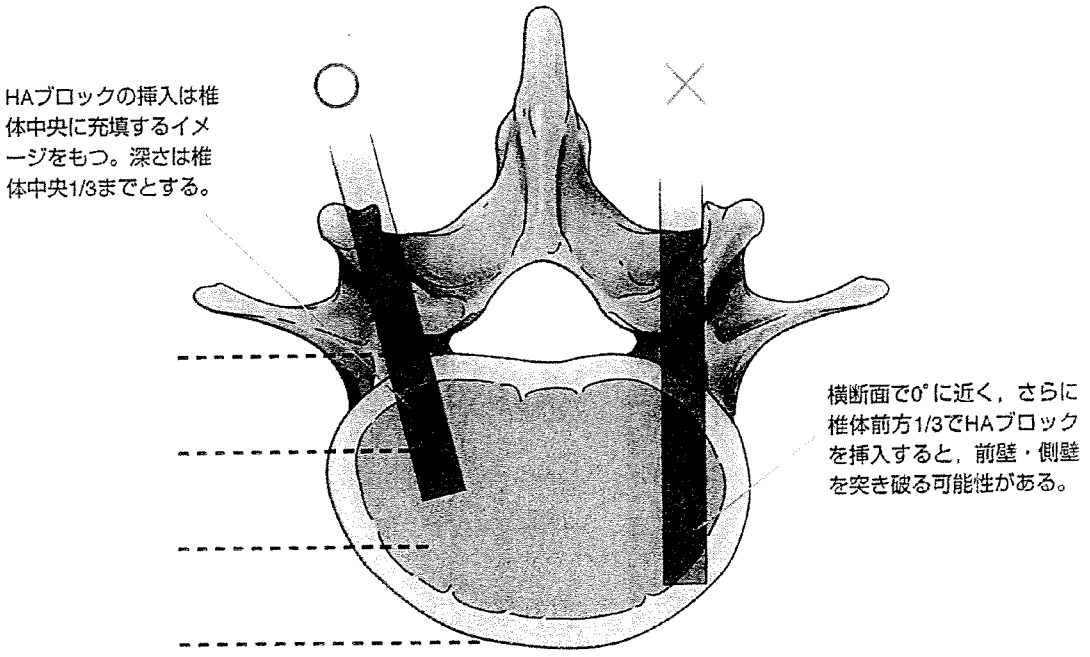

4 骨折部の整復・母床の作製 ヤマ

本法が成功するための重要な要素の1つは，椎体前方にうまく壁をつくることである。そのためには，椎体後方から中央の海綿骨を前方にていねいに圧縮させ，椎体前方に海綿骨の壁をつくるのが重要である(**図7**)。

手術のコツ，注意点

椎体内操作時の各種エレベータの使用時に，椎体前壁および側壁を壊さないことが最も重要である。そのためには，X線透視で得られる二次元の画像を常に三次元的に考えることが必要である。椎体中央部を整復するイメージで施行するとよい(**図6, 7**)。

5 HAブロックの充填

椎体整復およびエレベータで作製された充填スペースに，HAブロックを充填する。インサーターは，側面像で椎体中央1/3の深さに置き，椎体中央に充填するイメージでHAブロックを挿入する(**図6**)。用手的に入る限界までHAブロックを充填し，抵抗を感じるようになったらハンマーでインサーターの内筒を叩いて挿入する(**図8**)。その後は，3～5ケースHAブロックを充填したら，インパクターでHAブロックをしっかり打ち込む(**図8b**)。この操作を繰り返し，椎体後壁より約1cm手前まで充填されたら対側に移る。充填可能なHAブロックの数は通常25～40(平均30)ケース必要である。

図7 骨折部の整復

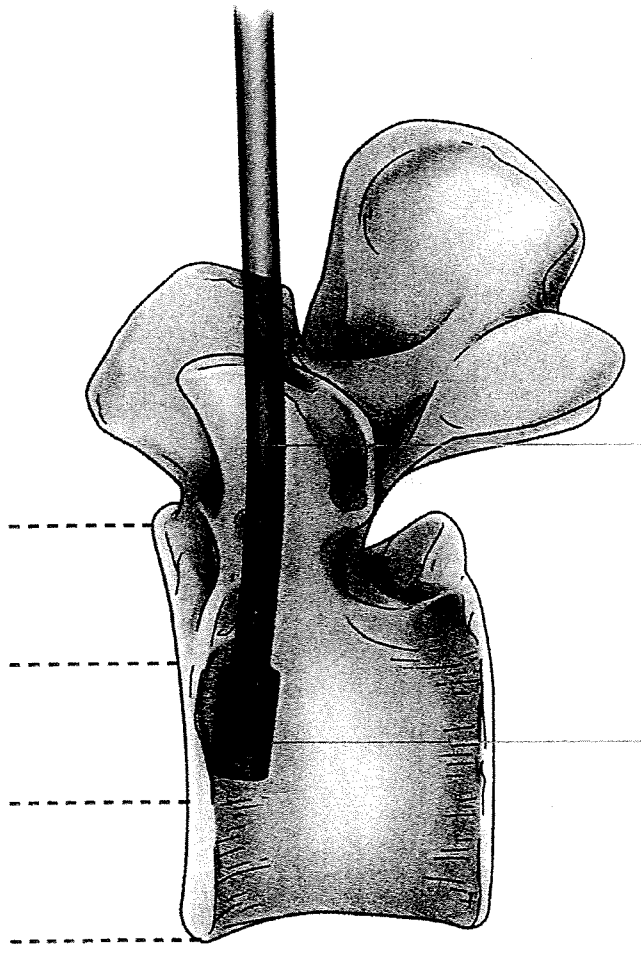

図8 HAブロックの充填

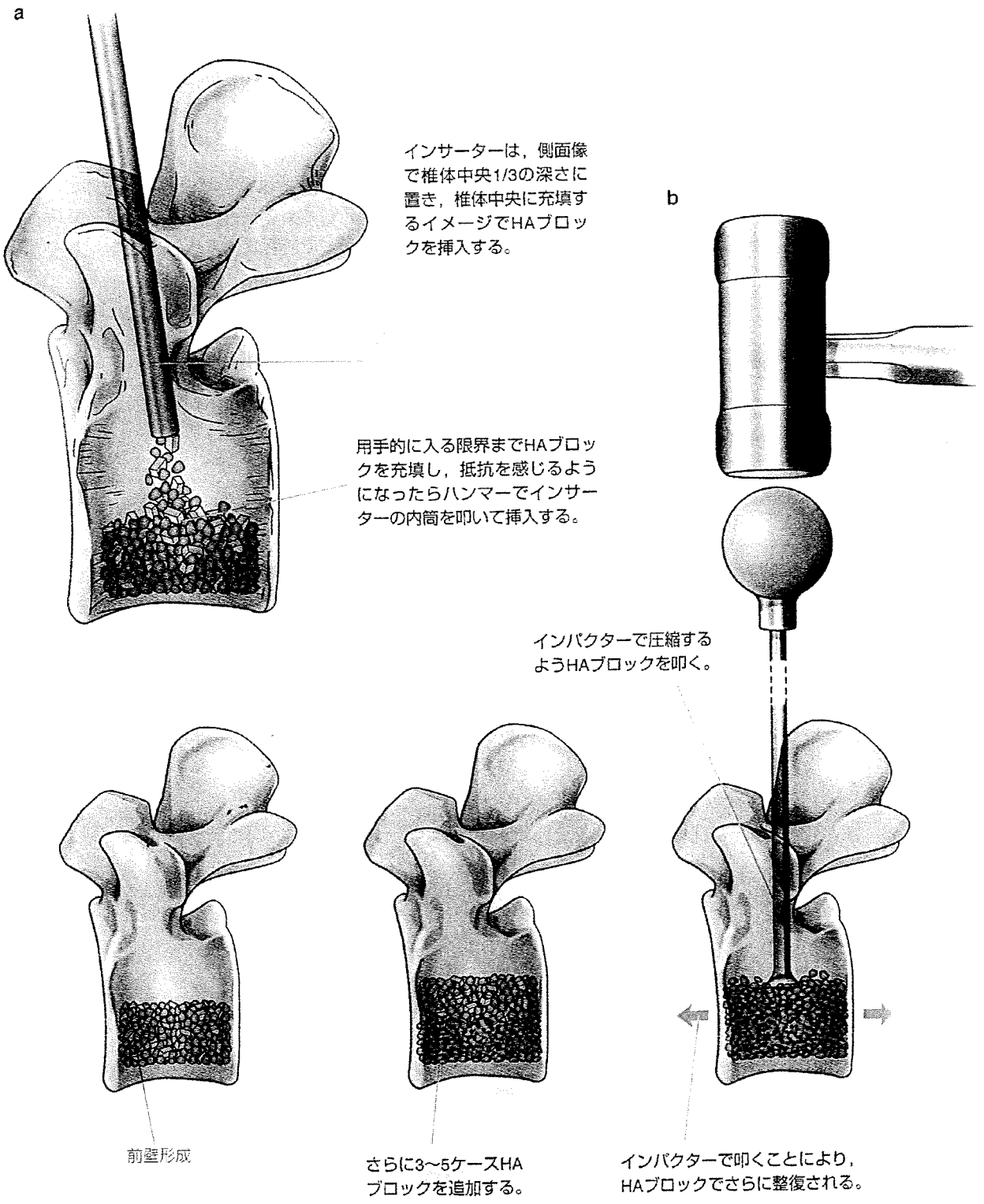

図9　インサーターの把持

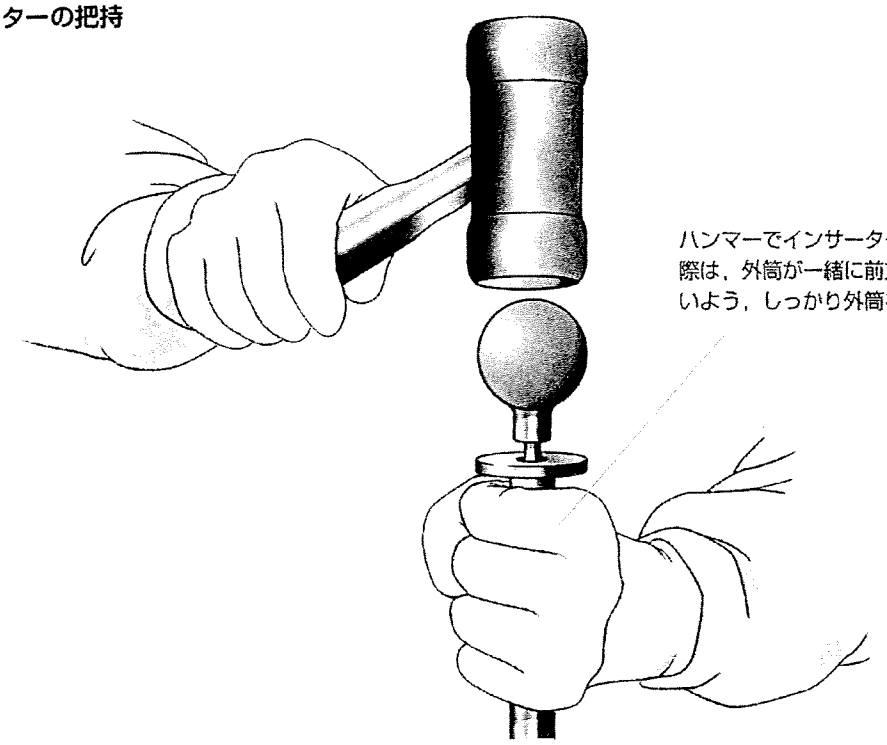

手術のコツ，注意点

インパクターの内筒を叩いてHAブロックを充填する際，外筒をしっかり保持し，外筒と内筒を一緒に打ち込まないこと（**図9**）。

トラブルシューティング

HAブロックが椎体外逸脱した！

X線透視で判明したらすぐに逸脱側の挿入を中止し，対側へHAブロックを挿入する。

6 椎弓根孔の閉鎖

HAブロックの椎弓根孔からの逸脱防止のため，HAプラグで閉鎖し，閉創する。閉創時のドレナージは不要である。

Repair of Large Osteochondral Defects in Rabbits Using Porous Hydroxyapatite/Collagen (HAp/Col) and Fibroblast Growth Factor-2 (FGF-2)

Hidetsugu Maehara,[1] Shinichi Sotome,[1,2] Toshitaka Yoshii,[1] Ichiro Torigoe,[1] Yuichi Kawasaki,[1] Yumi Sugata,[1,3] Masato Yuasa,[1,3] Masahiro Hirano,[4] Naomi Mochizuki,[4] Masanori Kikuchi,[5] Kenichi Shinomiya,[1,3,6,7] Atsushi Okawa[1]

[1]Department of Orthopaedic and Spinal Surgery, Graduate School, Tokyo Medical and Dental University, 1-5-45 Yushima, Bunkyo-ku, Tokyo 113-8519, Japan, [2]Development Division of Advanced Orthopaedic Therapeutics, Graduate School, Tokyo Medical and Dental University, 1-5-45 Yushima, Bunkyo-ku, Tokyo 113-8519, Japan, [3]Global Center of Excellence (GCOE) Program, International Research Center for Molecular Science in Tooth and Bone Disease, Tokyo Medical and Dental University, 1-5-45 Yushima, Bunkyo-ku, Tokyo 113-8519, Japan, [4]PENTAX New Ceramics Division, HOYA Corporation, 2-36-9 Maeno-cho, Itabashi-ku, Tokyo 174-8639, Japan, [5]Biomaterial Center, National Institute for Materials Science, 1-1 Namiki, Tsukuba, Ibaraki 305-0044, Japan, [6]Hard Tissue Genome Research Center, Tokyo Medical and Dental University, 2-3-10 Kanda-Surugadai, Chiyoda-ku, Tokyo 101-0062, Japan, [7]Core to Core Program for Advanced Bone and Joint Science, Tokyo Medical and Dental University, 2-3-10 Kanda-Surugadai, Chiyoda-ku, Tokyo 101-0062, Japan

Received 20 January 2009; accepted 14 September 2009
Published online in Wiley InterScience (www.interscience.wiley.com). DOI 10.1002/jor.21032

ABSTRACT: Articular cartilage has a limited capacity for self-renewal. This article reports the development of a porous hydroxyapatite/collagen (HAp/Col) scaffold as a bone void filler and a vehicle for drug administration. The scaffold consists of HAp nanocrystals and type I atelocollagen. The purpose of this study was to investigate the efficacy of porous HAp/Col impregnated with FGF-2 to repair large osteochondral defects in a rabbit model. Ninety-six cylindrical osteochondral defects 5 mm in diameter and 5 mm in depth were created in the femoral trochlear groove of the right knee. Animals were assigned to one of four treatment groups: porous HAp/Col impregnated with 50 μl of FGF-2 at a concentration of 10 or 100 μg/ml (FGF10 or FGF100 group); porous HAp/Col with 50 μl of PBS (HAp/Col group); and no implantation (defect group). The defect areas were examined grossly and histologically. Subchondral bone regeneration was quantified 3, 6, 12, and 24 weeks after surgery. Abundant bone formation was observed in the HAp/Col implanted groups as compared to the defect group. The FGF10 group displayed not only the most abundant bone regeneration but also the most satisfactory cartilage regeneration, with cartilage presenting a hyaline-like appearance. These findings suggest that porous HAp/Col with FGF-2 augments the cartilage repair process. © 2009 Orthopaedic Research Society. Published by Wiley Periodicals, Inc. J Orthop Res

Keywords: osteochondral repair; porous hydroxyapatite/collagen; fibroblast growth factor-2; scaffold; tissue engineering

Articular cartilage defects display a poor capacity for repair after injury because the tissue is avascular with a low level of mitotic cellular activity. Thus, damaged lesions in articular cartilage result in progressive deterioration and eventual osteoarthritis.[1] Several factors affect the healing process of these lesions. First, partial thickness defects that do not injure the subchondral bone display minimal healing. In contrast, full-thickness defects that penetrate the subchondral bone receive an abundant source of pluripotent marrow-derived mesenchymal cells for cartilage repair.[2] Second, fibrous or fibrocartilaginous tissues generally fill the defect site, and a limited amount of hyaline cartilage is found.

In recent years, several clinical methods have been used to repair cartilage lesions, including stimulation of the marrow by microfracture, mosaicplasty, and cell-based therapies. However, these methods have not always provided satisfactory results and have presented problems in clinical practice because the regenerated cartilage is morphologically, biochemically, and biomechanically inferior to the original cartilage.[3]

Various growth factors, including fibroblast growth factor-2 (FGF-2),[4] bone morphogenetic protein (BMP),[5–7] transforming growth factor-β (TGF-β)[8] and hepatocyte growth factor (HGF)[9] have also been applied to articular cartilage defects to promote repair. FGF-2 has received considerable attention because of its potential for clinical applications. FGF-2 is known as a chondrocyte mitogen [10] that is found in normal cartilage;[11] it can stimulate chondrocytes to synthesize cartilaginous matrix.[12,13] Although several studies have documented the utility of FGF-2 for cartilage repair,[15,16] disagreements exist regarding the effective doses for large osteochondral defect repair and FGF-2 carrier materials.

In our previous work, we developed a porous hydroxyapatite/collagen (HAp/Col) scaffold consisting of hydroxyapatite nanocrystals and type I atelocollagen.[17,18] The porous HAp/Col has the distinctive characteristics of bioabsorbability, elasticity, and excellent handling, and has been demonstrated to be a suitable material for use as a bone void filler and as a carrier of BMPs.[19–21] We hypothesized that porous HAp/Col with FGF-2 would accelerate subchondral bone repair when used to repair osteochondral defects, and that the local delivery of FGF-2 would promote cartilage repair compared to defects without treatment or defects treated with porous HAp/Col alone.

MATERIALS AND METHODS

Preparation of Porous HAp/Col

HAp/Col nanocomposite fibers were synthesized from atelocollagen derived from porcine skin, $Ca(OH)_2$ and H_3PO_4 using a coprecipitation method, according to a previous report by

Correspondence to: Shinichi Sotome (T: +81-3-5803-5272, F: +81-3-5803-5272; E-mail: sotome.orth@tmd.ac.jp)

Kikuchi et al.[17] In brief, a $Ca(OH)_2$ suspension and a H_3PO_4 solution containing type I atelocollagen (Nitta Gelatin Co., Osaka, Japan) were added to distilled water at 40°C, maintained at a pH of 9.0. The HAp/Col weight ratio was 80:20. The nanocomposite suspension was washed with distilled water and lyophilized.

Lyophilized composites (1 g) were homogenized with 6.5 ml of phosphate-buffered saline (PBS) and alkalized with 50 μl of 1 M sodium hydroxide solution. The solution was mixed with 1.5 ml of 0.6% collagen solution dissolved in phosphoric acid (pH 2.0). The resulting mixture was adjusted to pH 7.0 and infused into a mold. To initiate gelation of the collagen as a binder, the mold containing the mixture was incubated at 37°C for 2 h. The gelated HAp/Col was then frozen at −60°C. Freezing resulted in the growth of ice crystals, which were converted to pores by subsequent lyophilization. The lyophilized porous HAp/Col composite was cross-linked by thermal dehydration at 140°C for 12 h under vacuum and then cut into cylinders 5 mm in diameter and 3 mm in height (Fig. 1B). The porous HAp/Col composites were sterilized by gamma irradiation.

Surgical Procedures

All animal experiments were conducted according to the guidelines provided by the animal committee of the Tokyo Medical and Dental University. Ninety-six skeletally mature male Japanese white rabbits weighing 2.7–3.5 kg were used. The animals were anesthetized by intramuscular administration of medetomidine hydrochloride (0.5 mg/kg) and ketamine hydrochloride (25 mg/kg). Anesthesia was maintained by intramuscular injection at 30-min intervals of half doses of the above solution. The right knee was operated on under sterile conditions. After a medial parapatellar skin incision, the patella was dislocated laterally. One full-thickness cylindrical osteochondral defect, 5 mm in diameter and 5 mm deep, was created in the center of the trochlear groove of the femur using a trephine and a drill-bit with continuous saline irrigation (Fig. 1A). After all debris was removed by flushing with saline, the implants were transplanted. The implants were prepared as follows: Porous HAp/Col was impregnated with 50 μl of recombinant human FGF-2 solution (Kaken Pharmaceutical Co., Ltd., Tokyo, Japan) by pipette at a concentration of 10 or 100 μg/ml and incubated at 4°C for 24 h (FGF10 or FGF100 group); alternatively, porous HAp/Col was impregnated with 50 μl of PBS (HAp/Col group). The doses were determined according to previous reports.[14–16] All implants were placed at the subchondral bone level 2 mm beneath the surface of the adjacent cartilage to permit a good connection between the bone marrow and the cartilage defect (Fig. 1C). Defects without implants comprised the control group (defect group). The joint capsule, the fascial layer, and the skin were closed. After the operation, all rabbits were allowed to move freely in the cages, without any splints. Animals were sacrificed with an overdose of sodium pentobarbital at 3, 6, 12, or 24 weeks after the operation ($n = 6$ in each group).

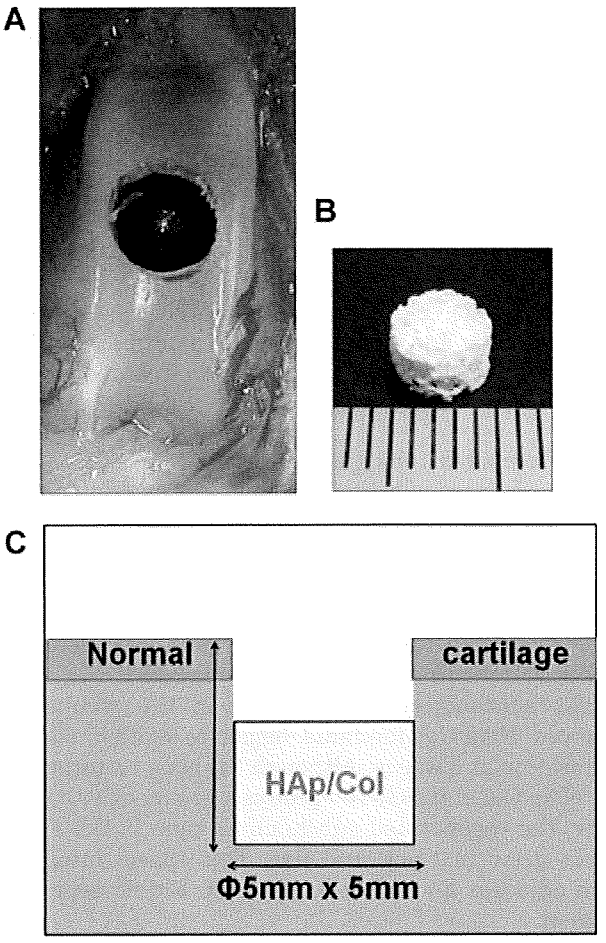

Figure 1. Surgical procedures: (A) Macroscopic observation of an osteochondral defect (5 mm in diameter and 5 mm in depth) in the patellar groove of the right distal femur; (B) cylindrical porous HAp/Col (5 mm in diameter and 3 mm in height) with or without FGF-2 was placed at the subchondral bone level; (C) illustration of the method used for transplantation.

Macroscopic Examination

The harvested knee joints were macroscopically assessed for adhesions, osteoarthritic changes, and synovitis. The appearance of the restored cartilage in terms of color, integrity, and smoothness was also examined. The distal femurs were resected and photographed.

Micro-Computed Tomography Images

To compare the subchondral bone regeneration in each group, the harvested tissues were evaluated with a micro-computed tomography (micro-CT) scanner (ScanXamte-E090, Comscantecno Co. Ltd., Tokyo, Japan). After scanning and reconstruction, each image was displayed in a sagittal view. Regenerated subchondral bone was quantitatively analyzed using bone analysis software (TRI/3D-BON, Ratoc System Engineering Co. Ltd., Tokyo, Japan). The volume of regenerated bone in the defect was quantified as a percentage of the total tissue volume of the defect.

Histological Examination

After fixation with 4% paraformaldehyde solution, the specimens were decalcified in 20% ethylenediaminetetraacetic acid solution and embedded in paraffin. Sections of 5 μm thickness were cut sagittally through the center of the defect site and were stained with either hematoxylin and eosin or with toluidine blue, or else were used for immunohistochemical examination.

Immunohistochemical Examination

Sections were stripped of paraffin using xylene and then dehydrated through graded alcohols. For antigen retrieval, the sections were pretreated with 0.4 mg/ml proteinase K (DAKO, Carpinteria, CA) in Tris-HCl for 15 min at room

temperature. Sections were then treated with 3% H_2O_2 for 15 min to quench endogenous peroxidase activity and incubated in PBS containing 10% normal horse serum at room temperature for 20 min to block nonspecific staining. Sections were then incubated with primary antibodies (mouse anti-human anti-type I and type II collagen; Daiichi Fine Chemical, Toyama, Japan) at room temperature for 1 h. The sections were treated with a secondary biotinylated horse anti-mouse IgG antibody (Vector Laboratories, Burlingame, CA) at room temperature for 30 min and immunostained with VECTASTAIN ABC reagent (Vector Laboratories) and diaminobenzidine. The slides were counterstained with Mayer's hematoxylin.

Histological Scoring

For semiquantitative analysis of the repaired tissue, histological sections were scored blindly by three expert observers according to a modified version of the histological grading scale, as described by Wakitani et al. [22] The scale consists of six categories (cell morphology, matrix staining, surface regularity, thickness of cartilage, regenerated subchondral bone, and integration with adjacent cartilage) scored on a scale from 0 to 16 points, where 16 denotes completely normal tissue (Table 1).

Table 1. Histological Scoring System

Category	Point
Cell morphology	
Hyaline cartilage	4
Mostly hyaline cartilage	3
Mostly fibrocartilage	2
Mostly non-cartilage	1
Non-cartilage only	0
Matrix-staining (metachromasia)	
Normal	3
Slightly reduced	2
Markedly reduced	1
No metachromatic staining	0
Surface regularity[a]	
Smooth	3
Moderate	2
Irregular	1
Severely irregular	0
Thickness of cartilage (%)[b]	
121–150	1
81–120	2
51–80	1
0–50	0
Regenerated subchondral bone	
Good	2
Moderate	1
Poor	0
Integration with adjacent cartilage	
Both edges integrated	2
One edge integrated	1
Neither edge integrated	0
Total maximum	16

[a]Total smooth area of the reparative cartilage compared with the entire area of the cartilage defect.
[b]Average thickness of the reparative cartilage compared with that of the surrounding cartilage.

Statistical Analyses

Histological scoring data and bone volume were analyzed using two-factor ANOVA followed by a multiple comparison test using the Tukey HSD test. Differences were considered statistically significant when the p-value was <0.05.

RESULTS

Macroscopic Observation

No joint contracture, infection, osteoarthritic change, or obvious synovitis was found in any rabbits.

At 3 weeks following injury (Fig. 2A), the regenerated defects in the HAp/Col and FGF10 groups began to fill with whitish opaque tissue from peripheral areas, although the regenerative areas were clearly distinguishable from the normal cartilage. In contrast, the defects in the defect and FGF100 groups remained almost empty, and the bottoms of the defects were covered with reddish granulated tissue.

At 6 weeks (Fig. 2A), larger portions of the defects in the FGF10 group were covered with white regenerated tissue extending from peripheral areas to the central portion. Cartilage regeneration in the FGF100 group was almost equal to that in the HAp/Col group, but was inferior to that in the FGF10 group. The defects in the defect group showed regeneration in the peripheral areas, but the reparative tissue surface was irregular and concave.

At 12 weeks (Fig. 2A), the newly formed tissue in the FGF10 group appeared glossy, smooth, and similar to neighboring normal cartilage. No obvious margins could be distinguished. The defects in the other groups were for the most part filled with whitish rough tissues or were sometimes concave.

At 24 weeks (Fig. 2A), the reparative tissue surface was glistening and smooth (similar to normal cartilage) in the FGF10 group, while it appeared white, opaque, and irregular in the other groups.

Micro-Computed Tomography Images

The regenerated subchondral bone was evaluated using micro-CT images in sagittal planes that passed through the center of the defect (Fig. 2A). Bone formation in the defect group was very poor up to 6 weeks after the operation. Even at 12 or 24 weeks, subchondral bone regeneration in the defect group was incomplete. The defect centers often remained unrepaired.

The subchondral bone defects in the groups that received HAp/Col implants began to exhibit signs of restoration at 3 weeks. Although the bone restoration in the HAp/Col and FGF100 groups were moderate thereafter, the regenerated subchondral bone in the FGF10 group grew in thick and flat. This tissue integrated with adjacent normal bone tissue in a time-dependent fashion.

Quantitative analysis of regenerated subchondral bone (Fig. 2B) showed that, in comparison to the defect group, significantly more subchondral bone was formed in the three groups that were implanted with HAp/Col (Fig. 2C). In particular, the bone volume in the FGF10

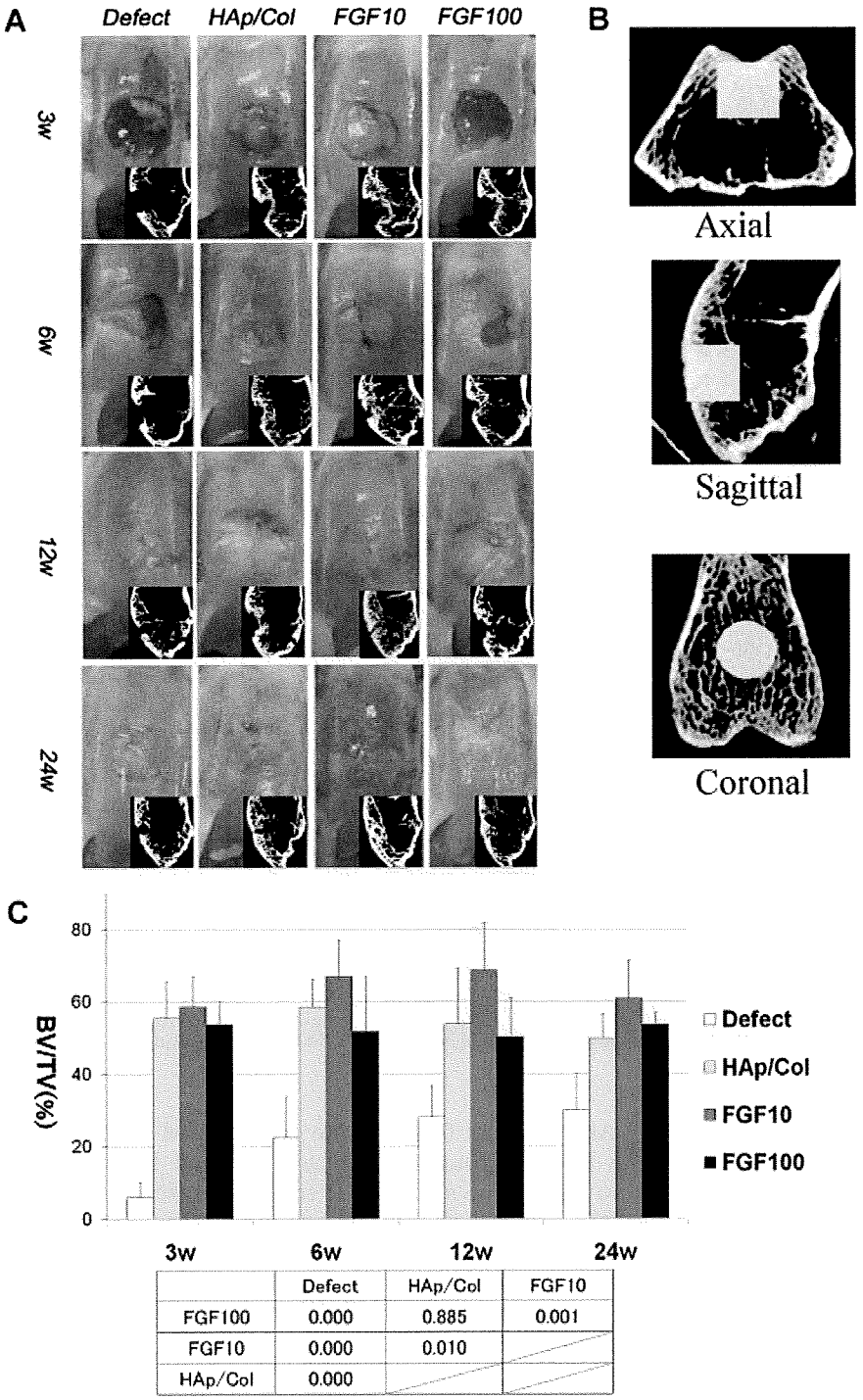

	Defect	HAp/Col	FGF10
FGF100	0.000	0.885	0.001
FGF10	0.000	0.010	
HAp/Col	0.000		

Figure 2. Representative macroscopic observation and micro-CT images of osteochondral defects: (A) Gross appearance and sagittally reconstructed micro-CT images of a representative specimen from each group at 3, 6, 12, and 24 weeks postoperatively; (B) reconstructed micro-CT images that were used to analyze bone volume defects (green areas of each plane); (C) ratios of regenerated bone volume (BV) to the tissue volume (TV) of the defects. The graph indicates mean values and standard deviations; *p*-values of overall data across all time points between each group are shown in the panel under the graph.

group was greater than the volume in the other three groups, and this finding was statistically significant.

Histological Observations

At 3 weeks (Fig. 3), the defects in the defect group were filled with fibrous tissue, no new bone formation was identified, and the cartilaginous extracellular matrix was very poorly developed. Restoration of the defects in animals implanted with HAp/Col with or without FGF-2 was more advanced than that of those in the defect group; notably, most of the implants persisted. The subchondral areas of the defects that were treated with HAp/Col were regenerated with new bone from the periphery of the implant. Superficial layers were also regenerated with cartilage-like tissue from the peripheral areas of the defects. Most importantly, the defects in the FGF10 group were filled with abundant new bone

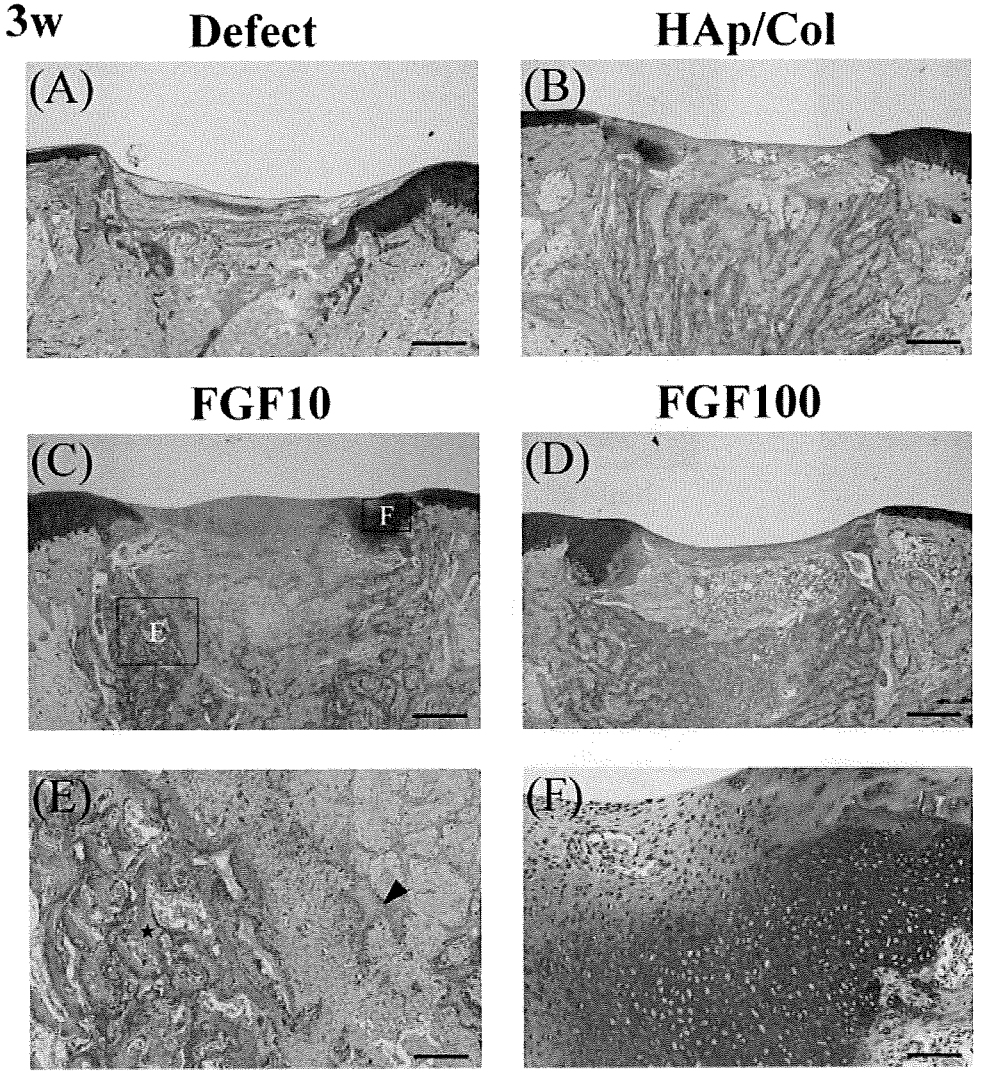

Figure 3. Histological observation at 3 weeks: Sagittal sections stained with toluidine blue taken from the defect group (A), HAp/Col group (B), FGF10 group (C), or FGF100 group (D). Panels (E) and (F) show the framed areas in panel (C) at higher magnification. In panel (E), the arrowhead indicates the remaining HAp/Col and the star indicates the newly formed bone. Scale bars represent 1 mm for (A–D), 300 μm for (E), and 125 μm for (F).

and cartilage matrix from the deep and peripheral areas.

At 6 weeks, the defects in each group improved as compared with those observed at 3 weeks. In comparison with other groups, the defects in the FGF10 group appeared to be satisfactorily regenerated. The tissue from the FGF10 group was primarily composed of round chondrocytes, and the matrix was more distinctly stained with toluidine blue, although fissures or concavities were sometimes observed.

At 12 weeks (Fig. 4), the repaired tissues in the defect, HAp/Col, and FGF100 groups were mainly fibrocartilaginous or fibrous with surface irregularities, and fissures or concave areas were frequently observed. In the FGF10 group, the defects were mostly filled with hyaline-like cartilage with a regular surface that was well-integrated with the native cartilage. An abundance of cartilage matrix could be identified by toluidine blue staining; immunostaining revealed the presence of type II, but not type I collagen. Continuous subchondral bone was well-formed, and the border between regenerated cartilage and subchondral bone was clear.

At 24 weeks (Fig. 5), the regenerated cartilage in the FGF10 group was densely stained by toluidine blue and by the anti-type II collagen antibody, but not by the anti-type I collagen antibody. The regenerated cartilage displayed a hyaline-like appearance with surface regularity and integration with the normal cartilage, whereas the defects in other groups still had not healed.

Histological Scores

The repaired tissue was assessed in a blinded manner by three observers using a modified version of Wakitani's grading scale. There were no significant differences in the scores obtained by the three observers (Fleiss' kappa score of total scores by the observers was 0.674). The histological scores of the FGF10 group improved continuously throughout the 24 weeks of the study, and the overall score of the FGF10 group across all time points was higher than those of all other groups (for each, $p < 0.05$; Fig. 6). Scoring rates in each category are shown in Table 2.

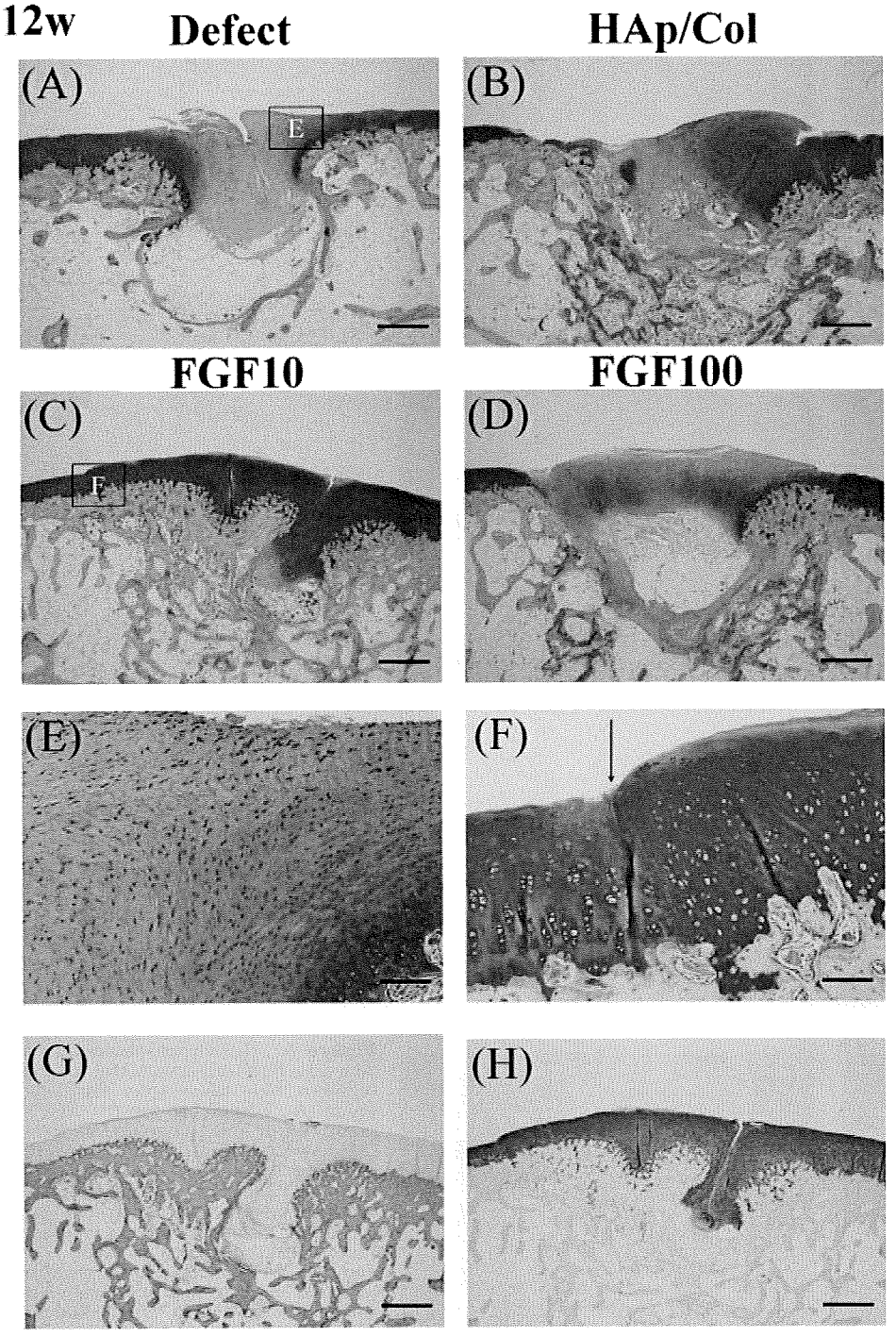

Figure 4. Histological observation at 12 weeks: Sagittal sections stained with toluidine blue taken from the defect group (A), HAp/Col group (B), FGF10 group (C), or FGF100 group (D). Panels (E) and (F) show the framed areas in panels (A) and (C) at higher magnification. The arrow in panel (F) indicates the boundary between newly formed cartilage and the surrounding native cartilage. Immunohistochemistry for type I (G) and type II (H) collagen in the regenerated tissue of the FGF10 group. Scale bars represent 1 mm for (A–D), (G) and (H), and 125 μm for (E) and (F).

DISCUSSION

This study investigated the effect of porous HAp/Col impregnated with FGF-2 on the restoration of large osteochondral defects in the rabbit model. Our results demonstrated the ability of porous HAp/Col in combination with a low dose of FGF-2 to repair osteochondral defects.

Regeneration of full-thickness cartilage defects is related to the size of the defect.[23,24] Smaller cylindrical full-thickness defects (3 mm) spontaneously regenerate articular cartilage. In contrast, larger defects (5 mm) result in the formation of fibrous scar tissue. This study established a new method for implanting porous HAp/Col impregnated with FGF-2 to repair the defect observed in a large (5 mm diameter) cylindrical full-thickness defect model.

Porous HAp/Col is a bone void filler that has high osteoconductivity, bioabsorbability, elasticity, and

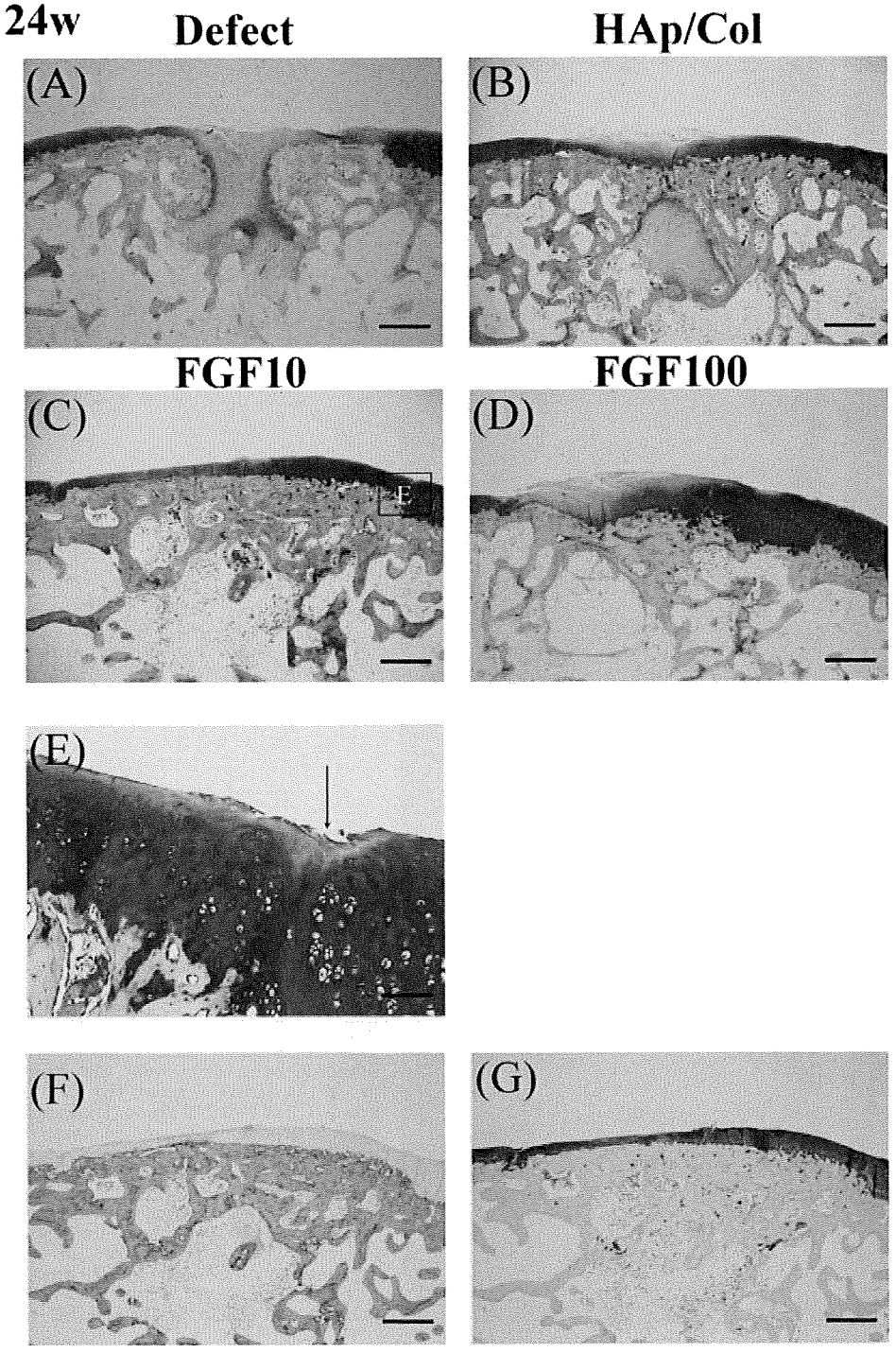

Figure 5. Histological observation at 24 weeks: Sagittal sections stained with toluidine blue taken from the defect group (A), HAp/Col group (B), FGF10 group (C), or FGF100 group (D). Panel (E) shows the framed area in panel (C) at higher magnification. The arrow in panel (E) indicates the boundary between newly formed cartilage and the surrounding native cartilage. Immunohistochemistry for type I (F) and type II (G) collagen in the repaired tissue of the FGF10 group. Scale bars represent 1 mm for (A–D), (F) and (G), and 125 μm for (E).

excellent handling. The material is highly porous (porosity: 95%), and the pore size (100–500 μm) is appropriate for bone formation. Due to these distinctive properties, we attempted to transplant the material into the subchondral bone level of the defect in order to promote bone repair. Bone formation was denser in the implanted HAp/Col groups than in the control group. The most abundant bone regeneration and the most satisfactory cartilage regeneration were obtained in the FGF10 group. According to previous reports[6,25] and, in accord with the correlation between cartilage repair and subchondral bone formation observed in our study, activation of the subchondral bone repair process probably enhanced the direct effects of FGF-2 on articular cartilage regeneration. Subchondral bone formation may have resulted from subchondral bone repair induced by the osteoconductive property of porous HAp/Col. Actively regenerating subchondral bone is likely to recruit additional pluripotent progenitor cells to the defect, demonstrating the concept of marrow

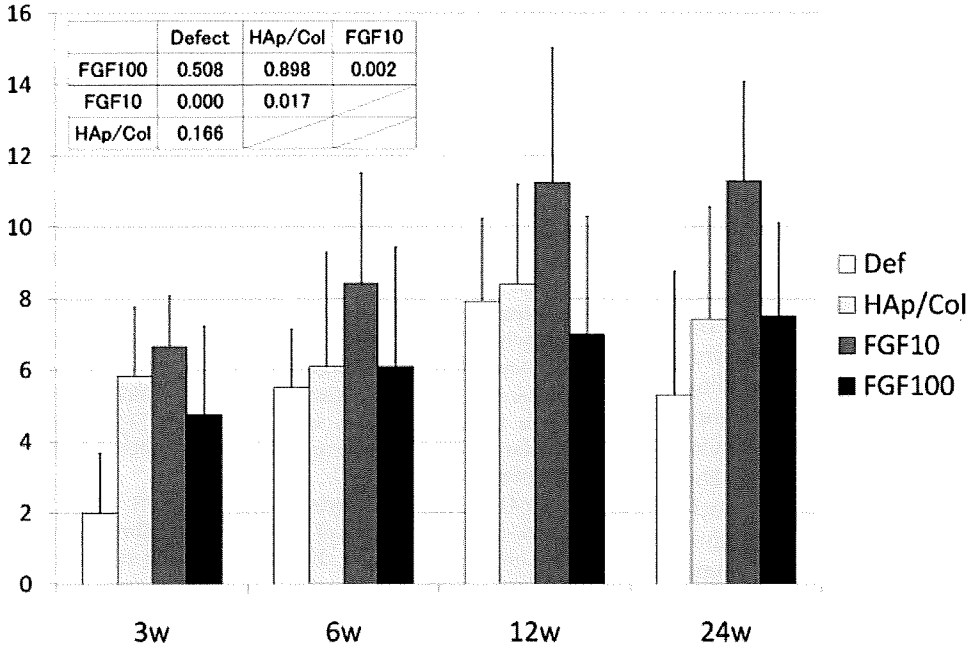

Figure 6. Histological scoring of the repaired tissue; histological findings were quantified using a scoring system (Table 1) where the score for normal cartilage was 16 points. The graph indicates mean values and standard deviations; *p*-values of overall scores across all time points between each group are shown in the panel included in the graph.

stimulation.[26,27] Alternately, factors secreted by actively regenerating cells in subchondral bone may exert paracrine effects on cartilage regeneration.

FGF-2 facilitates the synthesis of cartilaginous matrix by chondrocytes.[12,13] In the present study, although the basic HAp/Col transplant did not successfully result in full cartilage repair, HAp/Col impregnated with a low dose of FGF-2 promoted subchondral bone and cartilage regeneration. However, with a high-dose FGF-2, the regeneration of cartilage and its underlying subchondral area was poor. Biphasic dose-dependent responses are commonly observed in the context of growth factor biology.[28,29] High doses of FGF-2 may downregulate FGF receptors, reducing the growth factor's specific action. The FGF-2 doses used in this study were chosen based on previous reports.[14–16] There are some reports of successful osteochondral defect regeneration with a lower dose of FGF-2 than that used in our study.[30,31] The low-dose FGF-2 in our study demonstrated a superior improvement of osteochondral defect regeneration compared to the high-dose FGF-2. Lower-dose FGF-2 combined with porous HAp/Col, therefore, may be more effective for osteochondral regeneration.

Table 2. Scoring Rates in Each Category

		Scoring Rate (%) (SD)					
	Time (Weeks)	Cell Morphology	Matrix Staining	Surface Regularity	Thickness of Cartilage	Regenerated Subchondral Bone	Integration with Adjacent Cartilage
Defect	3	15.3 (12.3)	18.5 (16.7)	22.2 (17.2)	0.0 (0.0)	0.0 (0.0)	8.3 (20.4)
HAp/Col		30.6 (10.1)	37.0 (9.1)	42.6 (27.6)	13.9 (19.5)	47.2 (26.7)	47.2 (22.2)
FGF10		30.6 (10.1)	38.9 (13.6)	50.0 (18.3)	30.6 (24.5)	50.0 (0.0)	58.3 (20.4)
FGF100		30.6 (15.8)	25.0 (20.4)	38.9 (23.0)	8.3 (20.4)	52.8 (28.7)	30.6 (35.6)
Defect	6	33.3 (12.9)	33.3 (0.0)	51.9 (16.7)	16.7 (23.6)	13.9 (19.5)	44.4 (13.6)
HAp/Col		37.5 (13.7)	33.3 (21.1)	33.3 (29.8)	33.3 (25.8)	27.8 (25.1)	61.1 (25.1)
FGF10		50.0 (15.8)	50.0 (27.9)	44.4 (27.2)	50.0 (31.6)	66.7 (27.9)	63.9 (22.2)
FGF100		37.5 (13.7)	33.3 (21.1)	33.3 (29.8)	27.8 (25.1)	33.3 (40.8)	66.7 (25.8)
Defect	12	51.4 (16.2)	51.9 (16.7)	46.3 (16.4)	58.3 (18.6)	25.0 (23.0)	58.3 (20.4)
HAp/Col		43.3 (13.7)	40.0 (14.9)	60.0 (27.9)	50.0 (35.4)	56.7 (19.0)	76.7 (25.3)
FGF10		62.5 (20.9)	61.1 (25.1)	72.2 (32.8)	80.6 (24.5)	75.0 (27.4)	83.3 (25.8)
FGF100		48.3 (23.1)	44.4 (15.7)	33.3 (23.6)	43.3 (38.4)	30.0 (27.4)	60.0 (22.4)
Defect	24	31.7 (17.1)	33.3 (20.8)	33.3 (33.3)	30.0 (27.4)	30.0 (27.4)	36.7 (21.7)
HAp/Col		48.6 (14.4)	44.4 (17.2)	37.0 (21.8)	33.3 (40.8)	47.2 (26.7)	66.7 (38.0)
FGF10		65.0 (13.7)	60.0 (27.9)	71.1 (25.6)	70.0 (27.4)	90.0 (22.4)	80.0 (27.4)
FGF100		51.4 (12.3)	46.3 (16.4)	40.7 (19.5)	41.7 (20.4)	41.7 (34.6)	58.3 (20.4)

Our results also demonstrated the effectiveness of porous HAp/Col as an FGF-2 carrier. FGF 10 and 100 without HAp/Col groups were also tested although only three weeks post operatively. They did not show any improvement compared to the control at three weeks after the surgery. The release profile of FGF-2 from porous HAp/Col was also assessed. Although a precise release profile was not elucidated owing to rapid degeneration of FGF-2 dissolved in PBS, the assessment indicated that degeneration of FGF-2 adsorbed on HAp/Col was reduced compared to FGF-2 dissolved in PBS (data not shown) HAp/Col exhibits sponge-like hydrophilia, which are advantageous in a vehicle for drug delivery. Furthermore, because the HAp crystals contained in HAp/Col are on the nanoscale, porous HAp/Col has a high surface area, effectively promoting the absorption of molecules with an affinity for HAp, such as BMPs and TGF-β. Previous reports have demonstrated the usefulness of HAp/Col implants.[21,32,33] Some BMPs are known to facilitate cartilage regeneration,[5–7] preserve cartilage,[34,35] and promote chondrogenic differentiation of bone marrow stem cells.[36] Consequently, porous HAp/Col combined with BMPs in addition to FGF-2 may provide a means to repair osteochondral defects more successfully.

Prior to clinical application, further studies, including evaluation of the mechanical properties of regenerated cartilage, will be required to determine the optimal dose of FGF-2, the advisability of combination with other drugs, the particularities of various defect sizes, and the responses of different animals. Depending on the results of these studies, it may be possible to develop acellular treatments for chondral and osteochondral defects by using the porous HAp/Col as a scaffold and as a carrier for drug delivery.

In conclusion, we have successfully induced repair of large full-thickness osteochondral defects in a rabbit model using porous HAp/Col as a scaffold and a carrier for FGF-2, although further study is required to determine the optimal dose of FGF-2.

ACKNOWLEDGMENTS

This work was supported by a Grant-in-Aid for Scientific Research from the Ministry of Education, Culture, Sports, Science and Technology of Japan.

REFERENCES

1. Mandelbaum BR, Browne JE, Freddie F. 1998. Articular cartilage lesions of the knee. Am J Sports Med 26:853–861.
2. Shapiro F, Koide S, Glimcher MJ. 1993. Cell origin and differentiation in the repair of full-thickness defects of articular cartilage. J Bone Joint Surg [Am] 75-A:532–553.
3. Smith GD, Knutsen G, Richardson JB. 2005. A clinical review of cartilage repair techniques. J Bone Joint Surg [Br] 87-B: 445–449.
4. Fujisato T, Sajiki T, Liu Q, et al. 1996. Effect of basic fibroblast growth factor on cartilage regeneration in chondrocyte-seeded collagen sponge scaffold. Biomaterials 17:155–162.
5. Sellers RS, Peluso D, Morris EA. 1997. The effect of recombinant human bone morphogenetic protein-2 (rhBMP-2) on the healing of full-thickness defects of articular cartilage. J Bone Joint Surg [Am] 79:1452–1463.
6. Tamai N, Myoui A, Hirao M, et al. 2005. A new biotechnology for articular cartilage repair: subchondral implantation of a composite of interconnected porous hydroxyapatite, synthetic polymer (PLA-PEG), and bone morphogenetic protein-2 (rhBMP-2). Osteoarthritis Cartilage 13:405–417.
7. Cook SD, Patron LP, Salkeld SL, et al. 2003. Repair of articular cartilage defects with osteogenic protein-1(BMP-7) in dogs. J Bone Joint Surg [Am] 85-A(Suppl 3):116–123.
8. Holland TA, Bodde EW, Baggett LS, et al. 2005. Osteochondral repair in the rabbit model utilizing bilayered, degradable oligo(poly(ethylene glycol) fumarate) hydrogel scaffolds. J Biomed Mater Res A 75:156–167.
9. Wakitani S, Imoto K, Kimura T, et al. 1997. Hepatocyte growth factor facilitates cartilage repair. Full thickness articular cartilage defect studied in rabbit knees. Acta Orthop Scand 68:474–480.
10. Froger-Gaillard B, Charrier AM, Thenet S, et al. 1989. Growth-promoting effects of acidic and basic fibroblast growth factor on rabbit articular chondrocytes aging in culture. Exp Cell Res 183:388.
11. Gonzalez AM, Buscaglia M, Ong M, et al. 1990. Distribution of basic fibroblast growth factor in the 18-day rat fetus: localization in the basement membranes of diverse tissues. J Cell Biol 110:753–765.
12. Nimni ME. 1997. Polypeptide growth factors: targeted delivery systems. Biomaterials 18:1201–1225.
13. Kato Y, Iwamoto M, Koike T. 1987. Fibroblast growth factor stimulates colony formation of differentiated chondrocytes in soft agar. J Cell Physiol 133:491–498.
14. Fukuda A, Kato K, Masahiro H, et al. 2005. Enhanced repair of large osteochondral defects using a combination of artificial cartilage and basic fibroblast growth factor. Biomaterials 26: 4301–4308.
15. Fujimoto E, Ochi M, Kato Y, et al. 1999. Beneficial effect of basic fibroblast growth factor on the repair of full-thickness defects in rabbit articular cartilage. Arch Orthop Trauma Surg 119:139–145.
16. Miyakoshi N, Kobayashi M, Nozaka K, et al. 2005. Effects of intraarticular administration of basic fibroblast growth factor with hyaluronic acid on osteochondral defects of the knee in rabbits. Arch Orthop Trauma Surg 125:683–692.
17. Kikuchi M, Itoh S, Ichinose S, et al. 2001. Self-organization mechanism in a bone-like hydroxyapatite/collagen nanocomposite synthesized in vitro and its biological reaction in vivo. Biomaterials 22:1705–1711.
18. Rhee SH, Suetsugu Y, Tanaka J. 2001. Biomimetic configurational arrays of hydroxyapatite nanocrystals on bio-organics. Biomaterials 22:2843–2847.
19. Kikuchi M, Ikoma T, Syoji D, et al. 2004. Porous body preparation of hydroxyapatite/collagen nanocomposites for bone tissue regeneration. Key Eng Mater 254:561–564.
20. Yunoki S, Ikoma T, Tsuchiya A, et al. 2007. Fabrication and mechanical and tissue ingrowth properties of unidirectionally porous hydroxyapatite/collage composite. J Biomed Mater Res B Appl Biomater 80:166–173.
21. Sotome S, Orii H, Kikuchi M, et al. 2006. In vivo evaluation of porous hydroxyapatite/collagen composite as a carrier of OP-1 in a rabbit PLF model. Key Eng Mater 309-311:977–980.
22. Wakitani S, Goto T, Pineda SJ, et al. 1994. Mesenchymal cell-based repair of large, full-thickness defects of articular cartilage. J Bone Joint Surg [Am] 76:579–592.
23. Mizuta H, Kudo S, Nakamura E, et al. 2004. Active proliferation of mesenchymal cells prior to the chondrogenic repair response in rabbit full-thickness defects of articular cartilage. Osteoarthritis Cartilage 12:586–596.

24. Otsuka Y, Mizuta H, Takagi K, et al. 1997. Requirement of fibroblast growth factor signaling for regeneration of epiphyseal morphology in rabbit full-thickness defects of articular cartilage. Dev Growth Differ 39:143–156.
25. Huang X, Yang D, Yan W, et al. 2007. Osteochondral repair using the combination of fibroblast growth factor and amorphous calcium phosphate/poly(L-lactic acid) hybrid materials. Biomaterials 28:3091–3100.
26. Steadman JR, Rodkey WG, Rodrigo JJ. 2001. Microfracture: surgical technique and rehabilitation to treat chondral defects. Clin Orthop Relat Res 391(Suppl):S362–S369.
27. Yen YM, Cascio B, O'Brien L, et al. 2008. Treatment of osteoarthritis of the knee with microfracture and rehabilitation. Med Sci Sports Exerc 40:200–205.
28. Tanaka H, Mizokami H, Shiiji E, et al. 2004. Effects of basic fibroblast growth factor on the repair of large osteochondral defects of articular cartilage in rabbits: dose-response effects and long-term outcomes. Tissue Eng 10:633–641.
29. Aspenberg P, Thorngren KG, Lohmander LS. 1991. Dose-dependent stimulation of bone induction by basic fibroblast growth factor in rats. Acta Orthop Scand 62:481–484.
30. Chuma H, Mizuta H, Kudo S, et al. 2004. One day exposure to FGF-2 was sufficient for the regenerative repair of full-thickness defect of articular cartilage in rabbits. Osteoarthritis Cartilage 12:834–842.
31. Ishii I, Mizuta H, Sei A, et al. 2007. Healing of full-thickness defects of the articular cartilage in rabbits using fibroblast growth factor-2 and fibrin sealant. J Bone Joint Surg [Br] 89-B: 693–700.
32. Itoh S, Kikuchi M, Takakuda K, et al. 2002. Implantation study of a novel hydroxyapatite/collagen(HAp/Col) composite into weight-bearing sites of dogs. J Biomed Mater Res 63:507–515.
33. Sotome S, Uemura T, Kikuchi M, et al. 2004. Synthesis and in vivo evaluation of a novel hydroxyapatite/collagen-alginate as a bone filler and a drug delivery carrier of bone morphogenetic protein. Mater Sci Eng C 24:341–347.
34. Hayashi M, Muneta T, Ju YJ, et al. 2008. Weekly intra-articular injections of bone morphogenetic protein-7 inhibits osteoarthritis progression. Arthritis Res Ther 10:R118.
35. Badlani N, Inoue A, Healey R, et al. 2008. The protective effect of OP-1 on articular cartilage in the development of osteoarthritis. Osteoarthritis Cartilage 16:600–606.
36. Sekiya I, Colter DC, Prockop DJ. 2001. BMP-6 enhances chondrogenesis in a subpopulation of human marrow cells. Biochem Biophys Res Commun 284:411–418.